Poly(*p*-phenylene vinylene) light-emitting devices prepared via the precursor route onto indium tin oxide and fluorine-doped tin dioxide substrates

M. HEROLD, J. GMEINER, C. DRUMMER, M. SCHWOERER
Lehrstuhl für Experimentalphysik II, and Bayreuther Institut für Makromolekülforschung, Universität Bayreuth, 95440 Bayreuth, Germany

For the preparation of organic light-emitting devices (LEDs) an optically transparent and electrically conducting thin film is needed as anode. Usually, a glass substrate coated with indium tin oxide (ITO) is used. We show that ITO is unsuitable in the case of poly(*p*-phenylene vinylene) (PPV) prepared by the precursor route. We have found that a reaction in which hydrogen chloride is eliminated during the thermal conversion to PPV and the ITO takes place. Scanning electron microscopy investigations of the ITO–PPV interface demonstrates that indium chloride compounds, e.g., $InCl_3$ crystals with dimensions up to 40 μm, are produced. Photoluminescence measurements reveal that the fluorescence efficiency is quenched by a factor of 2–23 in the case of ITO compared with PPV converted onto usual glass. In a second step we have investigated LEDs prepared from PPV in the ITO/PPV/Al configuration in order to obtain information about the process responsible for the degradation of these devices. We shall show that the formation of the above-mentioned indium chloride compounds is one possible degradation mechanism and is responsible for the relative short lifetimes of these LEDs. To overcome this problem we propose to use fluorine-doped tin dioxide (FTO) instead of ITO. Finally, we show the results obtained for LEDs in the FTO/PPV/Al configuration and compare them with ITO/PPV/Al devices.

1. Introduction

Conjugated polymers are promising materials for the development of optoelectronic applications. They offer a large electrical conductivity upon doping [1–5] and exciting non-linear optical properties [6–8]. However, since the first publication about the conjugated polymer poly(*p*-phenylene vinylene) (PPV) as active layer in light-emitting diodes (LEDs) [9], many investigations have been performed concerning the electrical and optical properties of organic LEDs [10–12]. LEDs with large area both on glass [13, 14] and on flexible substrates [15] have been fabricated. The onset voltage of these devices is as low as 2 V [10, 16] and the colour can be tuned over a large range by polymer synthesis [17–21]. One limiting factor for these organic LEDs in industrial applications is the relative low quantum efficiency (normally 0.05% for indium tin oxide (ITO)/PPV/In devices) [22]. To overcome this problem, many groups have fabricated multilayer structures with electron- and/or hole-transporting layers between the cathode and the polymer and/or between the anode and the polymer, respectively. In these configurations both the quantum efficiency and the brightness of the devices increase [23–25]. Another possibility to enhance efficiency and brightness is to use metals with low work function as cathodes. For example, calcium instead of aluminium enhances the quantum efficiency by a factor of 10 [23]. However, the stability of Ca devices is much lower than those of Al devices. In our opinion, the most serious problem limiting most organic LEDs in industrial applications is their short lifetime. For PPV LEDs, for example, operating times up to 1000 h in an inert atmosphere have been reported [26], but these times are still too short for promising application.

In this paper we present investigations concerning the degradation process of PPV LEDs prepared by the tetrahydrothiophene precursor route. First, we have investigated the PPV–ITO interface and we found that the leaving group HCl interacts with ITO. We show that indium chloride compounds and even $InCl_3$ crystals with lateral dimensions up to 40 μm are created during the thermal conversion process. Secondly, we have investigated LEDs after operation and we found evidence that indium chloride is most probably one degradation mechanism of PPV LEDs. Quenching of the photoluminescence (PL) efficiency by a factor of up to 23 compared with PPV is observed if the elimination process is carried out on ITO-coated

0022–2461

substrates. To overcome both the reaction of HCl with ITO and the PL quenching we used glass substrates coated with fluorine-doped tin dioxide (FTO) as anode instead of ITO. Finally, we show the electrical and optical properties of LEDs in the FTO/PPV/Al configuration and compare them with the results of ITO/PPV/Al devices.

2. Experimental procedure

The tetrahydrothiophene polyelectrolyte precursor polymer was prepared according to the method published by Wessling [27]. Thin films of good optical quality were obtained with the doctor-blade technique [15] from a 0.05% pre-polymer solution. The conjugated material was obtained by successive thermal conversion. The temperatures and the conversion times are different for the various samples and are given for each investigated sample in the next section.

Scanning electron microscopy (SEM) and energy-dispersive X-ray analysis (EDXA) were carried out with a JEOL 840A on two kinds of sample. First, we used a PPV film approximately 5 μm thick which was prepared by dropping a concentrated solution of the pre-polymer onto a glass substrate coated with ITO. Further investigations were carried out on LEDs of PPV prepared in the usual configuration ITO/PPV/Al. The LEDs have been investigated after operation with current densities up to 200 mA cm^{-2} to ensure that the degradation processes have already started. The acceleration voltage during the SEM investigations was 10 kV.

The PL spectra were measured with a LS50B fluorescence spectrometer (Perkin–Elmer) and the current–voltage (I–V) characteristics were determined with a 237 source measurement unit (Keithley). The electroluminescence (EL) spectra were recorded with a liquid-nitrogen-cooled charge-coupled device camera (SI) combined with a monochromator and the EL quantum efficiency was measured with a calibrated Ulbricht sphere.

As anodes we used glass substrates coated with ITO or FTO with thicknesses of 100 nm and 300 nm, respectively. The ITO possess a sheet resistance of 30 Ω $\square^{-1}$, while the FTO coating has a sheet resistance of 17 Ω $\square^{-1}$.

3. Results

Fig. 1 shows the SEM image of a circular PPV film with a diameter of about 7 mm and a thickness of a few micrometres. The elimination process was carried out at 160 °C for 2 h in argon as exchange gas. As substrate we used glass coated with ITO. To obtain information about the ITO–PPV interface we peeled off the PPV film partially and tilted it back (compare Fig. 1). Further investigations were mainly carried out in regions A, B and C given in Fig. 1. From A we determined the composition of the ITO with EDXA and we found that the indium-to-tin ratio is about 85 to 10, which is in good agreement with other ITO samples [28, 29].

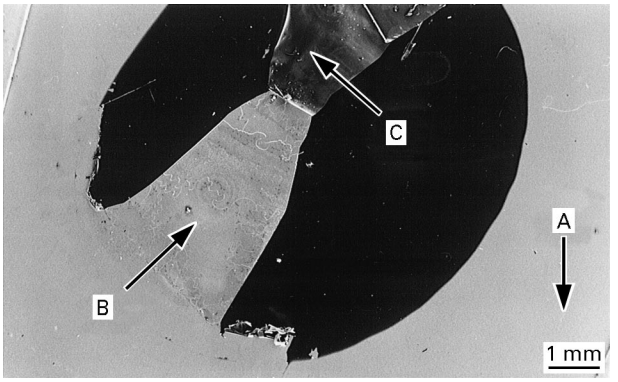

Figure 1 SEM image of a PPV film eliminated on ITO glass. A part of the film was peeled off and tilted back so that the regions A, B and C could be investigated in more detail.

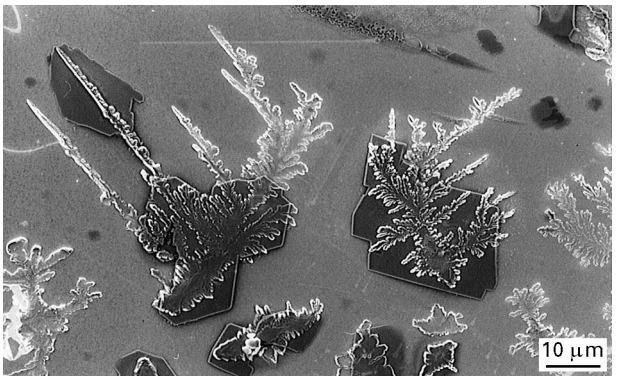

Figure 2 Part of region B (compare Fig. 1) where $InCl_3$ crystals have been found (black structures). The white branching structures are dendrites created by contact of the crystals with water.

Fig. 2 displays part of region B. Several large (up to 40 μm) crystals can be seen to appear black in the SEM image. The composition of the crystals was determined by EDXA and the data are shown in Fig. 3. As only chlorine at 2.8 keV and indium at 3.3 keV could be observed, we have determined the composition of the crystals. We found that they consist of 74 at% In and 26 at% Cl. This means that, during the thermal conversion of PPV, $InCl_3$ crystals are created at the PPV–ITO interface. A possible reaction scheme is given in the conclusion.

Fig. 2 is somewhat misleading owing to the black colour of the $InCl_3$ crystals in the SEM image. As can be seen in a light microscope the crystals are colourless as expected from [30]. Additionally, $InCl_3$ is hygroscopic and electrically conductive [30]. It is obvious that these two properties have crucial influences on the properties and operating times of LEDs. The white and strongly branching structures in Fig. 2 are dendrites. Contact with water will dissolve the $InCl_3$ crystals partially and subsequent fast crystallization yields dendrites which are much thinner than the $InCl_3$ crystals.

Images of the reverse side of the PPV film, i.e., parts of region C (see Fig. 1), are displayed in Fig. 4. The magnification is progressively enhanced from Fig. 4a to Fig. 4d. In Fig. 4a, several white regions can be

observed with a characteristic circular structure. One of these white structures is seen in Fig. 4b. The centre of this structure has an enhanced content of chlorine and indium compared with adjacent regions; however, we were not able to determine the exact composition with EDXA. Fig. 4c shows a part of the white structure with the centre at the left edge of the picture. Inside the dark circle in the right half of the image in Fig. 4c, toroidal deposits are observed while outside the deposits are sharper. A higher magnification of the toroidal deposits which have a diameter of approximately 3 μm is shown in Fig. 4d. EDXA yields for these structures enhanced amounts of sulfur, indium and tin compared with adjacent regions. We derive from the observations shown in Fig. 4 that the reaction of chlorine and indium or a subsequent reaction yields products for the interaction of sulfur and the ITO.

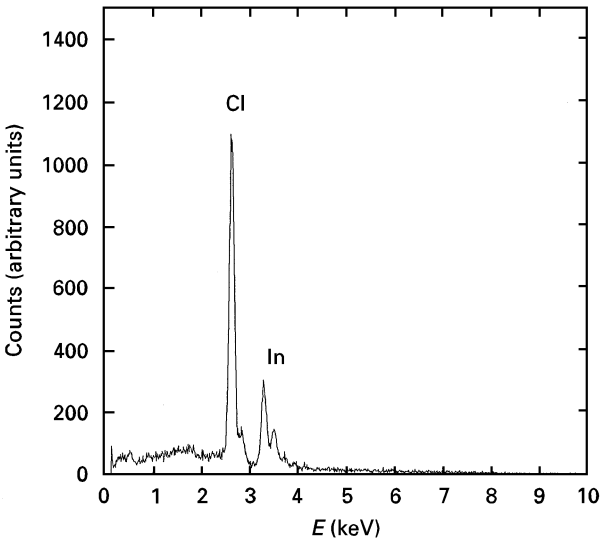

Figure 3 Energy-despersive X-ray spectrum of an $InCl_3$ crystal shown in Fig. 2.

Investigations concerning the degradation process of LEDs are much more difficult than the investigations shown so far as the aluminium electrode covers the active light-emitting area. However, we have obtained some SEM images concerning the degradation process. Together with EDXA we want to illustrate one possible mechanism that could be responsible for the short lifetime of the devices. For our investigations we used LEDs in the ITO/PPV/Al configuration which were driven at a relatively high current to ensure that the degradation process has already started. The active PPV layer has a thickness of about 100 nm and the elimination condition was 160 °C for 2 h in a vacuum of 10^{-3} mbar.

Fig. 5 shows an image of the LED from the top of the aluminium electrode. We observe many blisters created by gas evolution. The characteristic circular arrangement of the blisters has been observed for other samples, too, eliminated at temperatures lower than 160 °C as well as at higher temperatures (up to 300 °C). For most of the circular structures the aluminium electrode is damaged in the centre (Fig. 6). The centre of the structure is obviously one degradation mechanism of LEDs prepared from PPV. In another sample we observed a similar structure which seems to be in the initial stage. The EDXA yielded an enhanced chlorine amount and sometimes additionally sulfur compared with adjacent regions. It is surprising that

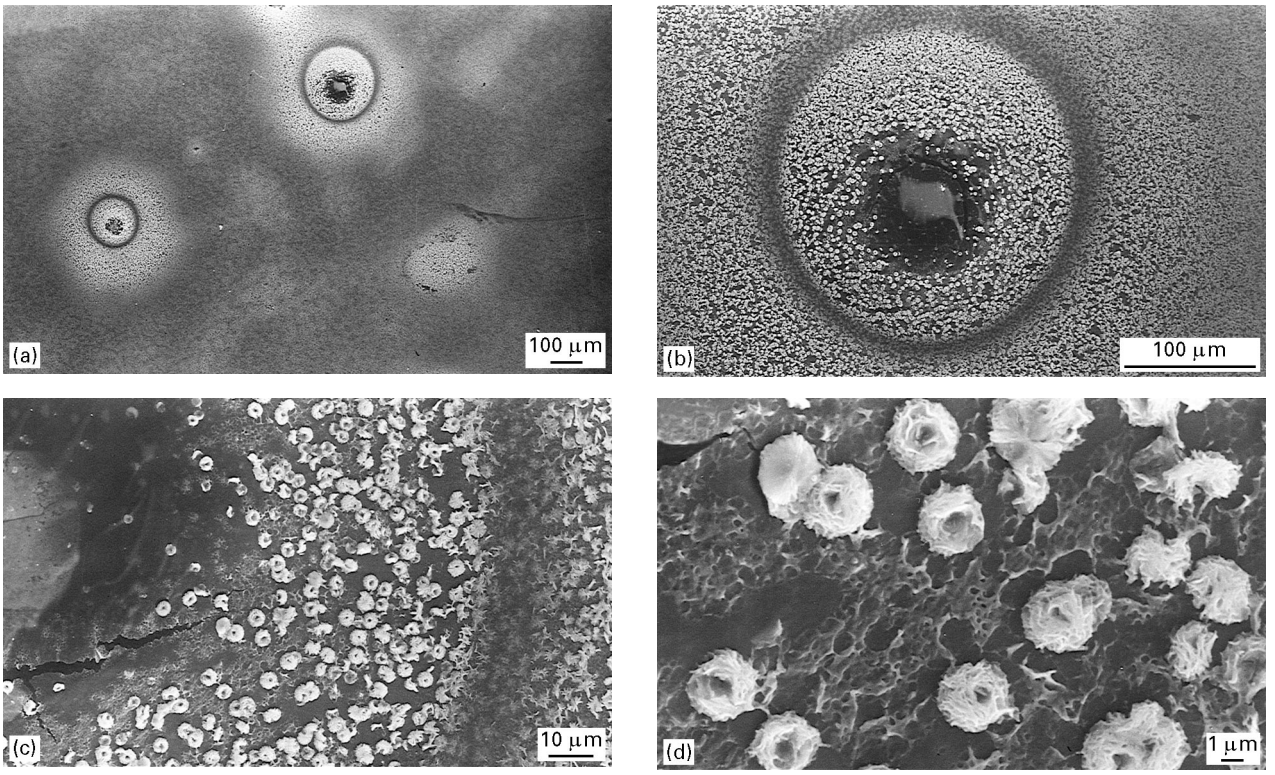

Figure 4 A view on the under side of the PPV film, i.e., region C in Fig. 1. The magnification was progressively enhanced from (a) to (d). For explanations see text.

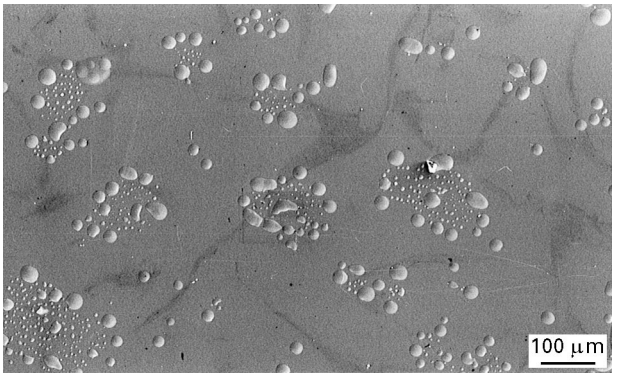

Figure 5 SEM image of an already driven LED prepared from PPV by looking onto the top of the aluminium electrode. Many-blisters can be observed resulting from gas evolution.

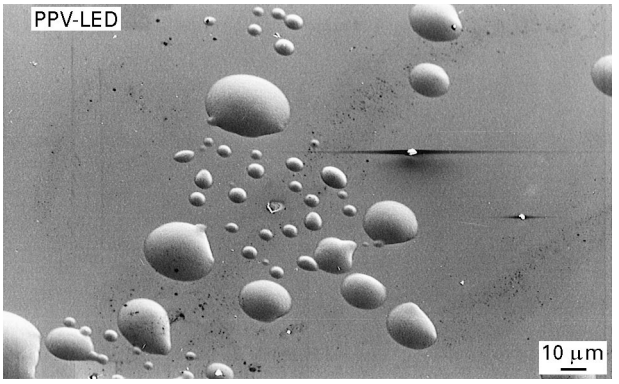

Figure 6 One of the structures in Fig. 5 at a larger magnification. In the middle the aluminium electrode is damaged.

for longer investigations with very large magnifications, i.e., strong increase in the sample temperature, the blisters are formed at the above-mentioned places during the SEM investigations. This is the reason why no image and no EDXA curve are shown in this paper.

Fig. 7 shows another centre where the aluminium is damaged but with the special feature that the cracked Al is located near the centre. We investigated three characteristic places denoted 1, 2 and 3 (see Figs 7 and 8). We have chosen this sample place as according to the geometry of 1 and 2 the upper side of 2 was formerly the under side of the Al electrode, i.e., we were able to investigate the interface between PPV and Al (compare the device structure given in Fig. 8). The energy-dispersive X-ray spectrum at 1 is displayed at the top in Fig. 8 and shows that mainly indium and tin are detected with a small amount of silicon and aluminium while, at 2, sulfur as well as chlorine can clearly be observed (Fig. 8, middle).

For comparison we have measured an energy-dispersive X-ray spectrum at 3 (Fig. 8, bottom). At 3, no sulfur and no chlorine could be observed although indium and tin from the ITO can be clearly measured. As sulfur and chlorine cannot be measured at 1 but are well resolved at 2 means that these atoms are inhomogeneously dispersed in the material, especially at the observed centres. The results given in Fig. 8 also

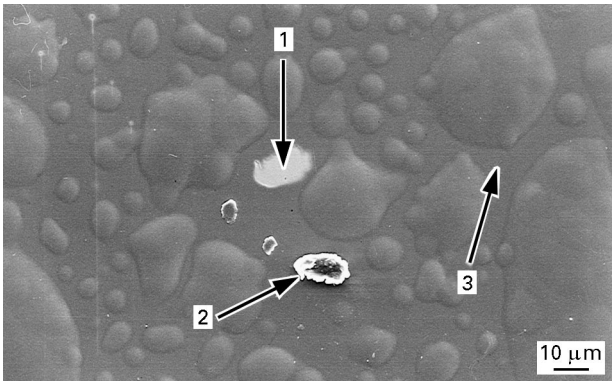

Figure 7 Centre of a structure in Fig. 5 where the cracked aluminium part lies next to the damaged place. Investigations were carried out at positions 1, 2 and 3. Compare the geometry of the cracked piece and the damaged part. The upper-side of 2 was formerly the under side of the aluminium coating.

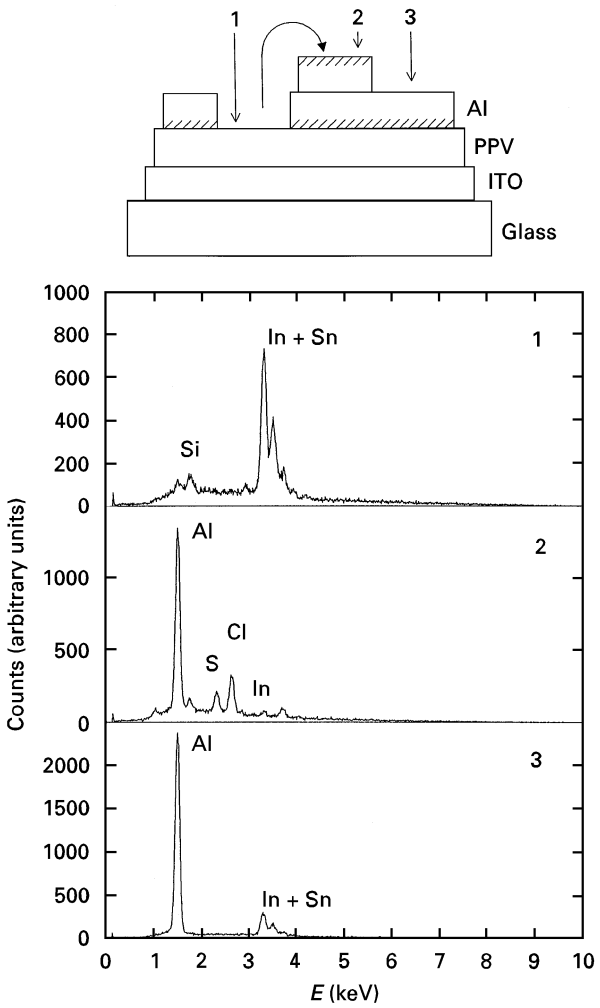

Figure 8 Energy-despersive X-ray spectra at 1, 2 and 3 concerning Fig. 7 together with the device structure (top).

show that the chlorine and sulfur released during the conversion to PPV are not removed completely and are located at certain places. These places are related to the centres of blisters observed as the degradation process in LEDs prepared from PPV. The results shown so far clearly demonstrate that substrates

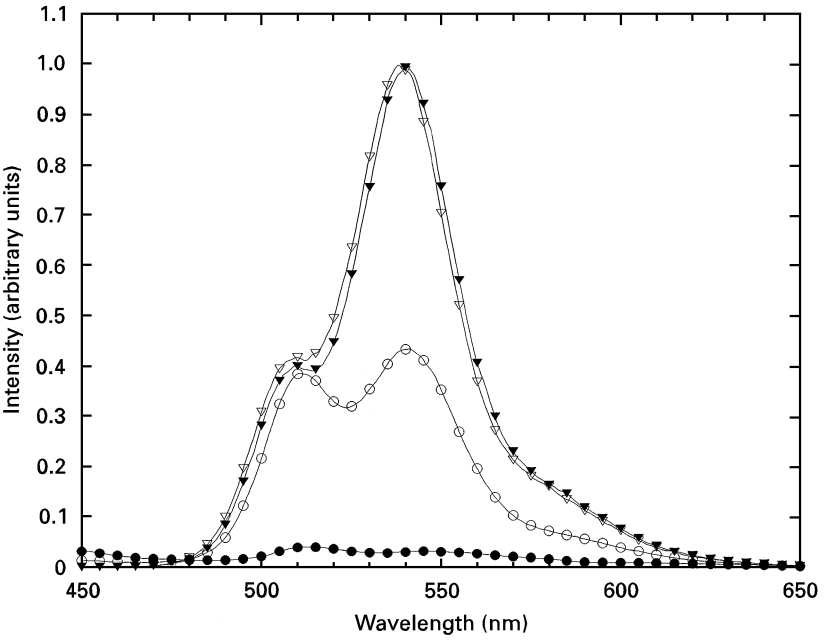

Figure 9 PL spectra of free-standing films of PPV eliminated on ITO and FTO, taken from various parts of the film. For the definition of top and back see text. (▽), FTO, top; (▼), FTO, back; (○), ITO, top; (●), ITO, back.

coated with ITO are unsuitable for the preparation of stable LEDs with PPV. To avoid a reaction of the elimination products with the anode during the thermal conversion we used a FTO coating instead of ITO.

Fig. 9 shows the PL spectra of free-standing films with a thickness of 600 nm eliminated on ITO and FTO. After the conversion process was carried out at 160 °C for 2 h in Ar, the films were removed from the coated substrates. As the PL spectra were recorded in reflection, parts of the removed film were turned around before they were put on a sample holder. This side of the film is termed the back in the following.

The two upper curves in Fig. 9 display the PL spectra of PPV eliminated on FTO and are taken from the top and the back of the film. No crucial difference in the spectra is observable while for PPV eliminated on ITO the PL spectra show quite distinct behaviours as for both the top and the back of the film the PL is reduced. For the top of the PPV film converted on ITO mainly the peak at 540 nm is quenched so that the peak at 510 nm is clearly resolved. This peak appears as a shoulder in the PL spectra of PPV converted on FTO. The most striking feature, however, is that nearly no PL light is detectable at the back of the film, i.e., at the PPV–ITO interface. A quantitative analysis yielded that the PL efficiency of the PPV film eliminated on ITO is 43.6% for the top and only 4.3% for the back, compared with the PL of PPV eliminated on FTO glass. Note that we have compared the PL of PPV converted on glass with PPV heated on FTO glass and we have found no difference in the spectra. The results obtain by PL spectroscopy have much crucial influence on the preparation and properties of PPV LEDs. First, the quenching of PL means that the EL efficiency is quenched, too. Secondly, the quenching sites are

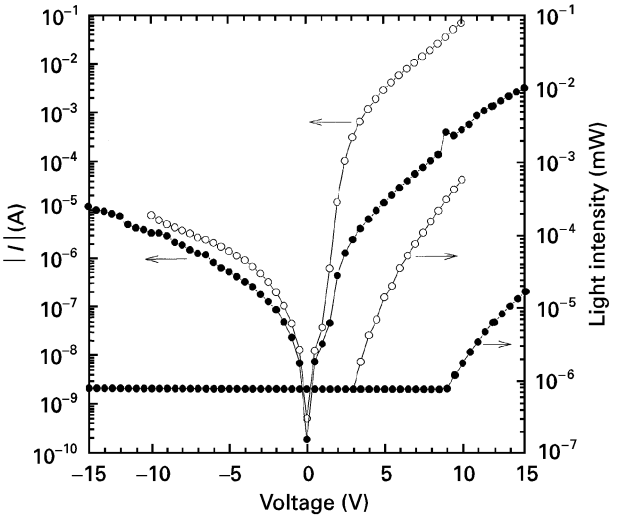

Figure 10 I–V characteristics and light outputs of ITO/PPV/AL (○) and FTO/PPV/Al (●) devices.

distributed in the whole film. As the absorption coefficient α is 3.5×10^5 cm^{-1} [15] at $\lambda_{exc} = 425$ nm, the penetration depth of the exciting light is 28 nm, which means that 99% of the incident light is absorbed in the first 130 nm of the film. Thirdly, one has to consider these results in the interpretation of the operation principle of PPV LEDs.

To overcome the reaction of HCl with ITO, the quenching of PL and the presented degradation mechanism of LEDs, we have prepared LEDs in the FTO/PPV/Al configuration and compared the results with ITO/PPV/Al LEDs fabricated in the same manner. The conversion of the PPV was carried out at 160 °C for 2 h in an Ar atmosphere and the film thickness of the PPV was 150 nm. Fig. 10 displays the

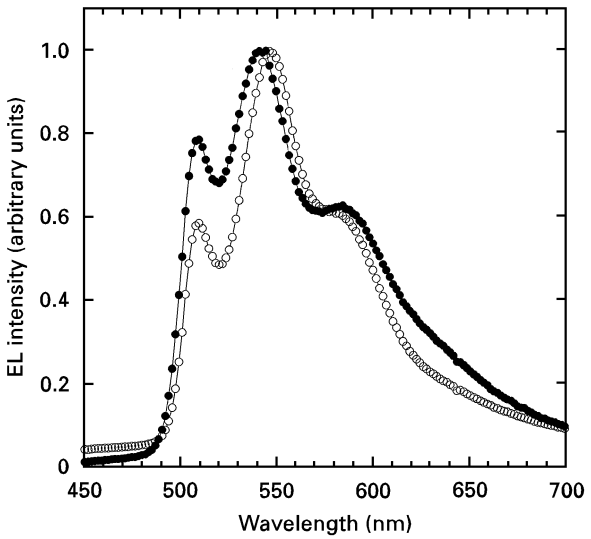

Figure 11 EL spectra of ITO/PPV/Al (○) and FTO/PPV/Al (●) devices.

I–V characteristic of the devices together with the light output. Both I–V characteristics possess a diode behaviour with increased current in forward direction, i.e., positive voltage in Fig. 10. However, the current through the ITO device is larger in both the backward and the forward direction compared with the FTO device. The largest discrepancies are the enhanced (up to two orders of magnitude) current in the forward direction of the ITO sample. While for the ITO/PPV/Al device light can be observed at a minimum voltage of $+3$ V, the threshold voltage for the FTO/PPV/Al device is drastically enhanced to $+9$ V. The brightness of both devices is approximately $1\,\mathrm{cd\,m^{-2}}$ and the external quantum efficiency is 0.0004% at $+10$ V and $+15$ V for the ITO and FTO LEDs, respectively. In Fig. 11 the EL spectra of the devices are compared. In contrast with the PL spectra both EL curves have nearly the same spectral shape with three peaks at 510, 545 and 585 nm.

4. Conclusion and summary

In summary, we have shown that the HCl released as elimination product reacts with the ITO coating. We have observed many small clusters containing a large amount of chlorine and indium compared with adjacent regions, and in the case of thicker PPV films even $InCl_3$ crystals with lateral dimensions up to 40 μm have been found. As $InCl_3$ is electrically conducting and hygroscopic, it will strongly influence the properties of LEDs prepared by PPV. We have also observed that sulfur crystals together with an enhanced amount of indium and tin were found around centres consisting of indium and chlorine. The observed indium chloride is most probably one possible degradation process for LEDs prepared from PPV, mainly owing to the following reasons. First, the observed gas evolution in the sample is distributed inhomogeneously, but always around centres that have an enhanced concentration of indium and chlorine. Second, as already noted, $InCl_3$ is electrically conductive which means that the electrical field in the device is inhomogeneously distributed, especially at the crystals. Therefore a large amount of the current will flow through the crystals and partially heat the device. The probability that gas is released at the crystals is enhanced owing to the large current densities.

In the following we want to propose the reaction of HCl on ITO during the conversion process. For the creation of the indium chloride compounds we have to consider the valence of indium. The relevant oxidized forms of indium are, for example, In_2O, InO and In_2O_3. The following reactions of the indium oxides with HCl are possible:

$$In_2O + 6HCl \rightarrow 2InCl_3 + H_2O + 2H_2\uparrow \quad (1)$$

$$In_2O_3 + 6HCl \rightarrow 2InCl_3 + 3H_2O \quad (2)$$

The reaction of InO with HCl which is not shown here will result in $InCl_2$ which can easily react to $InCl_3$ under the influence of HCl. The released hydrogen in reaction 1 plays an important role, as it can reduce In_2O_3:

$$In_2O_3 + 2H_2 \rightarrow In_2O + 2H_2O \quad (3)$$

This yields lower oxidized indium oxides. Further reductions are possible which can result in the creation of indium in its metallic form. Normally, In_2O_3 is the most stable oxidized form, but we believe that the ITO is not fully oxidized [31], which means that small amounts of In_2O and InO are sufficient to form $InCl_3$. We do not know the exact temperature required for reaction 3 but hydrogen even reduces SnO_2 which is more stable than In_2O_3 and forms tin at a temperture of 175–185 °C [32]. The reduction of SnO_2 to Sn explains the observed toroidal deposits consisting of sulfur, indium and tin (Fig. 4).

As $InCl_3$ is hygroscopic, it will contain most of the water created in reaction 1. The dendrites shown are due to contact of the $InCl_3$ crystals with water. This has a drastic influence on the operation of LEDs. Heating of the devices for example with a high current will vaporize the water. Consequently, blisters are formed in the LEDs during the operation. It is obvious that the operating times are drastically limited for PPV LEDs prepared on ITO.

To overcome these problems we propose to use FTO-coated glass substrates. Comparison of the results of ITO/PPV/Al and FTO/PPV/Al devices have shown that for the ITO sample the current is enhanced by up to two orders of magnitude while the onset voltage is much lower. Although the PL is drastically quenched by a factor of up to 23 for PPV converted on ITO-coated substrates, the EL quantum efficiency as well as the maximum brightness of the ITO/PPV/Al and FTO/PPV/Al devices are nearly the same. Additionally, the EL spectra are not influenced. We believe that indium chloride created during the conversion process on ITO acts as dopant for the PPV which explains the quenching of the PL and the large currents in this sample. As a further consequence the threshold voltage is reduced for ITO devices. Although the onset voltage in the case of FTO is higher than for

ITO as anode, we hope to fabricate more stable devices with FTO-coated substrates. Investigations concerning the operation times are under way.

Acknowledgements

We acknowledge Dr Bretschneider and Dr Hölscher (Flachglas AG) for offering us the FTO- and ITO-coated glass substrates and we are indebted to E. Werner for technical assistance and to Dr P. Strohriegl and Dr W. Rieß for stimulating discussions. We thank the Forschungsstiftung (Bayerische Forschungsverbund Optoelektronik: FOROPTO) and the Fonds der Chemischen Industrie for financial support.

References

1. R. MERTENS, P. NAGELS, R. CALLAERTS, M. VAN ROY, J. BRIERS and J. J. GEISE, *Synth. Metals* **51** (1992) 55.
2. R. W. LENZ, C. C. HAN, J. STENGER-SMITH and F. E. KARASZ, *J. Polym. Sci. A* **26** (1988) 3241.
3. I. MURASE, T. OHNISHI, T. NOGUCHI and M. HIROOKA, *Polym. Commun.* **25** (1984) 327.
4. T. OHNISHI, T. NOGUCHI, T .NAKANO, M. HIROOKA and I. MURASE, *Synth. Metals* **41–43** (1991) 309.
5. T. SCHIMMEL, W. RIEß, J. GMEINER, G. DENNINGER, M. SCHWOERER, H. NAARMANN and N. THEOPHILOU, *Solid State Commun.* **65** (1988) 1311.
6. F. KAJZAR and J. MESSIER, in "Conjugated polymers", edited by J. L. Bredas and R. Silbey (Kluwer, Deventer, 1991) p. 509.
7. H. S. NALWA, *Adv. Mater.* **5** (1993) 341.
8. T. KAINO and S. TOMARU, *ibid.* **5** (1993) 172.
9. J. H. BURROUGHES, D. D. C. BRADLEY, A. R. BROWN, R. N. MARKS, K. MACKAY, R. H. FRIEND, P. L. BURN and A. B. HOLMES, *Nature* **347** (1990) 539.
10. W. RIEß, S. KARG, V. DYAKONOV, M. MEIER and M. SCHWOERER, *J. Lumin.* **60–61** (1994) 906.
11. C. ZHANG, H. VON SEGGERN, B. KRAABEL, H.-W. SCHMIDT and A. J. HEEGER, *Synth. Metals* **72** (1995) 185.
12. Q. PEI and Y. YANG, *Adv. Mater.* **7** (1995) 559.
13. J. GMEINER, S. KARG, M. MEIER, W. RIEß, P. STROHRIEGL and M. SCHWOERER, *Acta Polym.* **44** (1993) 201.
14. M. SCHWOERER, *Phys. Blätter.* **1** (1994) 52.
15. M. HEROLD, J. GMEINER and M. SCHWOERER, *Acta. Polym.* **45** (1994) 392.
16. D. R. BAIGENT, N. C. GREENHAM, J. GRÜNER, R. N. MARKS, R. H. FRIEND, S. C. MORATTI and A. B. HOLMES, *Synth. Metals* **67** (1994) 3.
17. P. L. BURN, A. KRAFT, D. R. BAIGENT, D. D. C. BRADLEY, A. R. BROWN, R. H. FRIEND, R. W. GYMER, A. B. HOLMES and R. W. JACKSON, *J. Amer. Chem. Soc.* **115** (1993) 10117.
18. P. L. BURN, A. B. HOLMES, A. KRAFT, D. D. C. BRADLEY, A. R. BROWN, R. H. FRIEND and R. W. GYMER, *Nature* **356** (1992) 47.
19. W. TACHELET, S. JACOBS, H. NDAYIKENGURUKIYE, H. J. GEISE and J. GRÜNER, *Appl. Phys. Lett.* **64** (1994) 2364.
20. J. KIDO, M. KIMURA and K. NAGAI, *Science* **267** (1995) 1332.
21. E. Z. FARAGGI, H. CHAYET, G. COHEN, R. NEUMANN, Y. AVNY and D. DAVIDOV, *Adv. Mater.* **7** (1995) 742.
22. D. BRAUN and A. J. HEEGER, *Appl. Phys. Lett.* **58** (1991) 1982.
23. E. BUCHWALD, M. MEIER, S. KARG, P. PÖSCH, H.-W. SCHMIDT, P. STROHRIEGL, W. RIEß and M. SCHWOERER, *Adv. Mater.* **7** (1995) 839.
24. H. SUZUKI, H. MEYER, S. HOSHINO and D. HAARER, *J. Appl. Phys.* **78** (1995) 2684.
25. J. POMMEREHNE, H. VESTWEBER, W. GUSS, R. F. MAHRT, H. BÄSSLER, M. PORSCH and J. DAUB, *Adv. Mater.* **7** (1995) 551.
26. W. RIEß, S. KARG, M. MEIER, M. CÖLLE and J. GMEINER, in Technical Digest of the International Symposium on Inorganic and Organic Electroluminescence, 1994 (Hamamatsu, Tottori University, Tottori, 1994) p. 84.
27. R. A. WESSLING, *J. Polym. Sci., Polym. Symp.* **72** (1985) 55.
28. J. R. BELLINGHAM, W.A. PHILLIPS and C.J. ADKINS, *J. Phys.: Condens. Matter* **2** (1990) 6207.
29. J. C. C. FAN, *Appl. Phys. Lett.* **34** (1979) 515.
30. A. F. HOLLEMAN and E. WIBERG, "Lehrbuch der Anorganischen Chemie" (Walter de Gruyter, Berlin, 1985) p. 891.
31. K. L. CHOPRA, S. MAJOR and D. K. PANDYA, *Thin Solid Films* **102** (1983) 1.
32. L. GMELIN, "Gmelins Handbuch der anorganischen Chemie" (Chemie Weinheim, Weinstrasse, 1971) System-Nr. 46, Teil C1, 98.

Received 2 July 1996
and accepted 1 May 1997